ELSEVIER

Journal of Chromatography A, 760 (1997) 71–79

JOURNAL OF CHROMATOGRAPHY A

# Models for polybutadiene pore wall coatings in porous zirconia

David H. Reeder[a,c], Jianwei Li[b], Peter W. Carr[b,c], Michael C. Flickinger[c,d], Alon V. McCormick[a,*]

[a]*Department of Chemical Engineering and Materials Science, University of Minnesota, 421 Washington Ave S.E., Minneapolis, MN 55455, USA*

[b]*Department of Chemistry, University of Minnesota, 421 Washington Ave S.E., Minneapolis, MN 55455, USA*

[c]*Institute for Advanced Studies in Bioprocess Technology, St. Paul, MN 55108, USA*

[d]*Department of Biochemistry, University of Minnesota, St. Paul, MN 55108, USA*

**Abstract**

We present three models of the changes in measured pore size distribution for cylindrical pores when a polymer is deposited in the pores by evaporation from a volatile solvent. The predicted results serve as an aid in interpreting experimental nitrogen adsorption data for polybutadiene (PBD) coatings on porous zirconia. At low loadings, PBD appears to deposit in thin layers on the surface with no preference for filling either large or small pores. At higher PBD loadings, the polymer deposits preferentially in smaller pores. This is in qualitative agreement with PBD coatings on porous silica.

*Keywords:* Zirconia; Polybutadiene coatings; Coating; Stationary phases, LC

## 1. Introduction

The immobilization on silica gels of nonpolar polymers including polybutadiene (PBD), polystyrene, perfluoropolymers and polysiloxanes has been used as a method to make a wide range of packing materials for reversed-phase liquid chromatography [1,2]. Compared with typical reversed-phase materials such as silica gel chemically bonded with alkylsilane groups, silica supports modified with nonpolar polymers have enhanced stability at high pH and practically no silanophilic interactions with strongly basic compounds [3]. These properties make such materials suitable for separations of peptides, drugs and other compounds without complicated ion-pairing techniques. Alumina coated with hydrophobic polymer by the same procedures as those used for silica have even higher stability (pH 3–12) in alkaline solution than for silica [4,5].

Although alumina and silica are more stable in alkaline solution when coated with polymer, zirconia is a better choice as a support material than either alumina or silica [6,7]. Not only does zirconia have the desirable physical and mechanical properties of silica, but its chemical and thermal stability is superior to any other current support. These unique properties of zirconia have motivated us to develop zirconia-based supports. Over the past few years, we have been interested in a variety of chromatographic modes based on modified zirconia, including size-exclusion, ion-exchange and reversed-phase [8–12]. Rigney et al. [13] found that PBD-coated zirconia was stable in alkaline solution —there was no evidence for degradation of the support even after exposure to 1 *M* sodium hydroxide at 100°C— and columns of PBD-coated zirconia demonstrated quite reasonable reduced plate heights. More recently,

*Corresponding author.


*PII* S0021-9673(96)00623-1

PBD-coated zirconia has been effectively used to separate peptides and proteins in very acidic conditions, and the columns can be completely recovered by washing with concentrated acid and base [14,15]. All these results suggest that there is considerable potential to develop a better reversed chromatographic phase based on microparticulate zirconia.

In reversed-phase chromatography, retention increases with the amount of the hydrophobic phase; thus, from the standpoint of retention alone, it is desirable to have the PBD loading as high as possible. However, chromatographic efficiency is also dependent on mass transfer to and diffusion within the stationary phase [16,17]. Chromatographic data suggest that using the coating procedure described below diffusion within the particles (as evaluated by the $C$ term in the Knox equation) is significantly decreased at loadings above about 0.03 g PBD/g $ZrO_2$, thereby lowering the efficiency [18]. We would like to understand how the polymer fills the pore space, with the aim of adapting the coating procedure to achieve higher polymer loadings without deleterious effects on intraparticle diffusion.

We present here three simple models of polymer deposition within a porous media. They represent limiting cases for the distribution of polymer between pores of different sizes and for the conformation adopted within the pore by the polymer. These models predict how the pore size distributions would change in ideal systems if the polymer ends up filling the pore space in defined ways, and the results will aid in interpreting the experimental nitrogen adsorption data. The models do not include a mechanistic description of how the polymer reaches its final state, although each for each model one or mechanisms can be proposed.

Nitrogen adsorption and desorption data have been widely used to estimate pore size distributions; adsorption data is considered to reflect the size distribution of pore bodies and desorption data to represent the size distribution of pore throats (constrictions). Pore size distributions calculated from these data are based upon the assumption that the pore structure is a collection of unconnected cylindrical capillaries [19,20]; the models developed here are based on the same premise. Changes in the connectivity of the pore network, while of critical importance in chromatography [21–23], are not readily measurable by nitrogen adsorption and not determinable with these models.

The three models are depicted in Fig. 1. In the first model, the polymer forms uniformly smooth layers on the surface of the pores with the thickness of the layer being the same for all pores. In the second model, the polymer again forms a smooth layer on

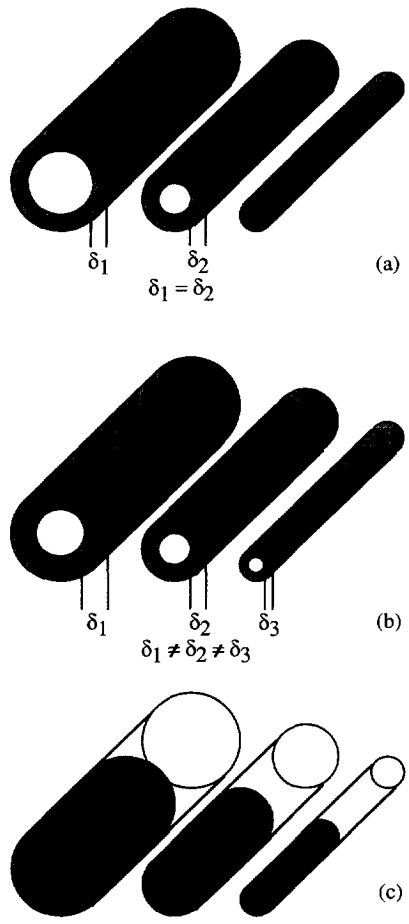


Fig. 1. Depiction of models for polymer within cylindrical pores. (a) The polymer forms a smooth layer of uniform thickness, $\delta$, on the walls of all pores. If the diameter of a given pore is less than $2\delta$, the pore is completely filled. (b) The polymer forms a smooth layer on the walls of all pores, but the thickness of the layers is not uniform for all pores. Instead, the volume fraction of polymer is uniform. (c) The volume fraction of polymer is uniform for all pores, but the polymer does not form a layer on the surface. Instead, the polymer forms a plug, decreasing the volume of the pore without changing the diameter.

the surface of the pore, but the thickness of the layer in a given pore is proportional to the cross-sectional area of the pore. This is equivalent to saying that the concentration (mass/volume) of polymer is the same for all pores. In the third model, the polymer is again distributed throughout the pores on the basis of pore volume, but rather than forming a smooth layer on the surface, the polymer forms a plug or cap.

## 2. Experimental

Zirconia particles (2.5–3 μm diameter, 30 $m^2/g$ surface area) were synthesized in our laboratory by polymerization-induced colloid aggregation (batch PICA-7). The post-synthetic treatment involves heating the particles under vacuum at 170°C for 24 h followed by pyrolysis in air at 375°C for 2 h to remove the urea-formaldehyde polymer binder. Particles were then sintered at 750°C for 6 h and at 900°C for 3 h. Finally the sintered particles were washed in 0.5 *M* nitric acid and then 0.5 *M* sodium hydroxide for 8 h.

Our method for preparing PBD coatings on chromatographic zirconia has been previously described [13,24]. Particles were dried under vacuum for 16 h at 120°C and cooled over phosphorus pentoxide. Solutions of 0.5–8% (w/v) molecular mass 5000 PBD in hexane were added to the particle. The slurry was sonicated under vacuum for 10 min to displace air within the pores with liquid; it was then gently swirled for at least 8 h. The crosslinking agent dicumyl peroxide was added to the slurry as a 0.05% (w/v) solution in hexane to a ratio of 2.5% (w/w) dicumyl peroxide/PBD. This mixture was sonicated and swirled for an additional hour, after which the solvent was evaporated over the course of 90 min by applying low vacuum at 35°C. The polymer was thermally crosslinked in a vacuum oven at 120°C for 1 h and 160°C for 4 h. Finally, the particles were extracted with toluene (110°C for at least 8 h) and washed with hexane to remove any free polymer.

The pore structures were characterized after heating the samples for 8 h at 150°C at $10^{-3}$ Torr (1 Torr=133.322 Pa) to remove surface contaminants. Nitrogen sorption was performed using a Micromeritics ASAP 2000 sorptometer (Micromeritics, Norcross, GA, USA). Approximate pore size distributions were calculated from nitrogen adsorption data using the BJH method [19,20]. The distributions are approximate since the method treats the pore structure as a collection of unconnected cylinders. Calculations from the models are based on nitrogen adsorption data for the uncoated zirconia particles.

## 3. Models

As an initial approximation, we assume that the pores are straight unconnected cylinders. We further assume that the density of the PBD (expressed as its inverse, the specific volume, $\bar{V}_{PBD}$) is a constant value of 0.89 $g/cm^3$. Thus the final total pore volume, $V_1$, is the difference between the initial total pore volume, $V_0$, and the volume occupied by the polymer for a given polymer loading, $W$ (g PBD/g $ZrO_2$).

$$V_1 = \frac{V_0 - \bar{V}_{PBD} W}{1 + W} \tag{1}$$

The pore size distributions $\partial V_1/\partial D$ and $f_V(a)$ are defined by their relations to the total pore volume.

$$V_1 = \int_0^\infty \left(\frac{\partial V_1}{\partial D}\right)_{D=d} \partial d = \int_0^\infty f_V(a)\, \partial a \tag{2}$$

These pore size distribution functions are equivalent and differ only in that one is expressed in terms of the diameter of uncoated pores, $a$, and the other in terms of the diameter of coated pores, $d$. For generality, $d$ is treated as a function of $a$. Based on the assumption that pores are cylindrical, the volume and area distributions are related by Eq. (3).

$$f_A(a) = 4\frac{f_V(a)}{d(a)} \tag{3}$$

From these equations we see that the pore volume distribution function describes how the polymer distributes through the pore space and that the pore area distribution function—through its inverse dependence on the pore diameter—describes how the polymer occupies a pore, e.g. whether or not the polymer changes the size of the pore.

In plots where, due to the large range, diameter is plotted on a logarithmic scale, it is common to plot $\partial V/\partial \log D$ rather $\partial V/\partial D$. By doing so, the area under

the curve is still proportional to the total pore volume. These functions for the pore volume and pore area distributions can be converted into distributions $g_V(a)$ and $g_A(a)$.

$$g_V(a) = f_V(a) \cdot d(a) \cdot \log(10) \tag{2a}$$

$$g_A(a) = f_A(a) \cdot d(a) \cdot \log(10) \tag{3a}$$

### 3.1. Model 1: uniform, smooth coating

Assuming the final polymer layer is of thickness $\epsilon/2$, the pore diameter is given by

$$d(a) = 0; \quad a < \epsilon \tag{4a}$$

$$d(a) = a - \epsilon = \left(1 - \frac{\epsilon}{a}\right)a; \quad a \geq \epsilon \tag{4b}$$

For the assumed cylindrical pores, the volume distribution function becomes

$$f_V(a) = 0; \quad a < \epsilon \tag{5a}$$

$$f_V(a) = \frac{\left(1 - \frac{\epsilon}{a}\right)^2}{1 + W} \left(\frac{\partial V_0}{\partial D}\right)_{D=a}; \quad a \geq \epsilon \tag{5b}$$

Since a pore cannot contain a polymer layer thicker than half its diameter, an iterative solution is needed for $\epsilon$ at higher polymer loadings. As smaller pores fill completely, the remaining polymer is distributed among the larger pores for conservation of the polymer. At each iteration step $V_1$ and $\partial V_1/\partial \epsilon$ are determined by integrating Eq. (2) and Eq. (6), respectively by the trapezoid method.

$$\frac{\partial V_1}{\partial \epsilon} = \frac{\partial}{\partial \epsilon}\left[\int_{\epsilon}^{\infty} \frac{\left(1 - \frac{\epsilon}{a}\right)^2}{1 + W} \left(\frac{\partial V_0}{\partial D}\right)_{D=a} \partial a\right]$$

$$= \int_{\epsilon}^{\infty} \left(\frac{-2}{1 + W}\right)\left(1 - \frac{\epsilon}{a}\right)\left(\frac{\partial V_0}{\partial D}\right)_{D=a} \partial a \tag{6}$$

$$\frac{V_0 - \bar{V}_{PBD} W - V_1(1 + W)}{\left(\frac{\partial V_1}{\partial \epsilon}\right)} = \Delta\epsilon \tag{7}$$

### 3.2. Model 2: volume proportional loading, smooth coating

In expressing our assumption that the concentration of the polymer is uniform throughout the pore space, we will define $S$, the fraction of the pore space that is filled by polymer.

$$S \equiv \frac{\bar{V}_{PBD} W}{V_0} = \frac{\left(\frac{\partial V_0}{\partial D}\right)_{D=a} - \left(\frac{\partial V_1}{\partial D}\right)_{D=a}}{\left(\frac{\partial V_0}{\partial D}\right)_{D=a}} \tag{8}$$

It follows that the pore volume distribution is given by Eq. (9).

$$f_V(a) = \left(\frac{1 - S}{1 + W}\right)\left(\frac{\partial V_0}{\partial D}\right)_{D=a} \tag{9}$$

In this model we assume that the polymer lies in a smooth annular layer on the surface. Thus the filled fraction of the pore is given by Eq. (10).

$$S = \frac{a^2 - d^2}{a^2} = 2\left(\frac{\epsilon(a)}{a}\right) - \left(\frac{\epsilon(a)}{a}\right)^2 \tag{10}$$

The change in pore diameter is given by Eq. (11).

$$d(a) = a - \epsilon(a) = \left(1 - \frac{\epsilon(a)}{a}\right)a = (\sqrt{1 - S})a \tag{11}$$

### 3.3. Model 3: volume proportional loading, plug coating

In this model, the polymer is again distributed proportionally through the pore space. The volume distribution is therefore again described by Eq. (8) and Eq. (9). However, rather than flattening on the surface, the polymer forms a bead or plug which does not change the pore diameter.

$$d(a) = a \tag{12}$$

## 4. Results and discussion

In Fig. 2, we have plotted the experimentally determined pore volume and pore area distributions of zirconia at several PBD loadings. At lower loadings (<0.025 g PBD/g $ZrO_2$), the shape of the pore size distributions are almost independent of the amount of polymer loaded except for a slight shift of

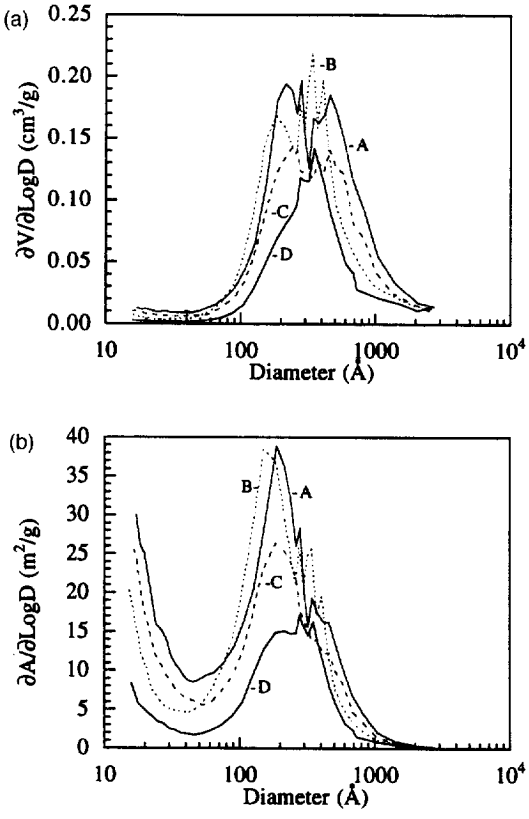


Fig. 2. Differential pore volume (a) and pore area (b) distributions for PBD-coated zirconia at several polymer loadings as calculated by the BJH method from nitrogen adsorption data. Polymer loadings are expressed as g PBD/g $ZrO_2$: (A) 0, (B) 0.018, (C) 0.031, (D) 0.068.

peaks towards smaller pore diameters. There is some variability in the heights of the peaks due to the fact that the distributions are determined by numerically differentiating discrete data; however, the integral over a finite section of the distribution is accurate. For higher loadings, the volume contribution of small pores (<400 Å) decreases more rapidly than larger pores, but the smaller pores never completely disappear. This suggests that the decrease in chromatographic efficiency at high velocities seen with higher loadings is due to the plugging of the narrower pore throats within the particles [7], lowering the connectivity of the pores. These results are qualitatively consistent with experimental results of PBD coating on silica [14].

Fig. 3 summarizes the total pore surface area as

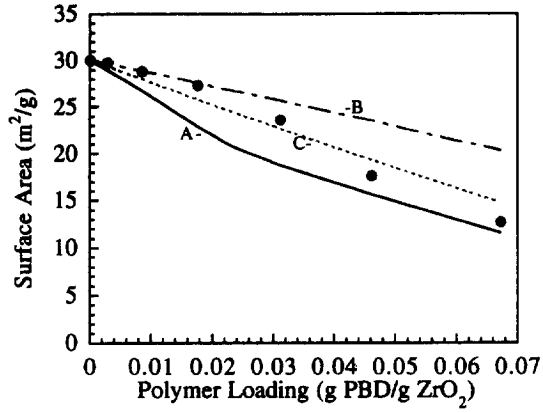


Fig. 3. Comparison of cumulative surface area against polymer loading. The solid circles represent experiments. The curves represent the changes predicted by the models: (A) uniform thickness–smooth (model 1), (B) uniform volume fraction–smooth (model 2) and (C) uniform volume fraction-plug (model 3).

determined by numerically integrating $dA/dD$ over the full range of discrete data points from experiment and models. The experimental pore areas decrease linearly with PBD loading up to loadings of about 0.025 g PBD/g $ZrO_2$; at higher loadings, the surface area decreases more rapidly. Models 2 and 3 each exhibit a linear decrease of area with PBD loading, but the slopes are different. Under model 1, the rate of surface area loss is greatest at low loadings, corresponding to the rapid volume loss of smaller pores which contribute significantly to the surface area. There is a strong correspondence between the data and the predictions of model 2 for loadings up to 0.025 g PBD/g $ZrO_2$. At higher loadings, the data seem to be approaching the values predicted by model 3. Our data differ slightly from those of Hanson et al. [25] for silica. They report that the measured surface area decreases linearly with PBD loading over the full range of their study (0–0.3 g PBD/g $SiO_2$) and conclude that the PBD is always forming plugs (e.g. model 3), but as seen in Fig. 3, other distributions of the polymer (e.g. model 2) can also produce a linear relation between surface area and polymer loading. The discrepancy between the results may be explained by the fact that pore sizes reported in their silica gel were more uniform (100–500 Å) than those in our porous zirconia (20–3000 Å); thus the ratio of the contributions to surface area

and pore volume for a pores of a given size would be more nearly constant across the range of pore sizes.

In Figs. 4–6 we have plotted pore volume and pore area distributions for the three models presented above; these are plots of $g_V(a)$ and $g_A(a)$ vs. $d(a)$ on a logarithmic scale and represent what would be expected experimentally for systems of unconnected cylindrical capillaries with defined polymer occupancies. When the polymer distributes on a volume proportional basis (models 2 and 3), the general shape of the pore volume distribution does not change — the volume contribution decreases equally rapidly for pores of all sizes. However, a shift in peaks toward lower pore diameters is seen when the

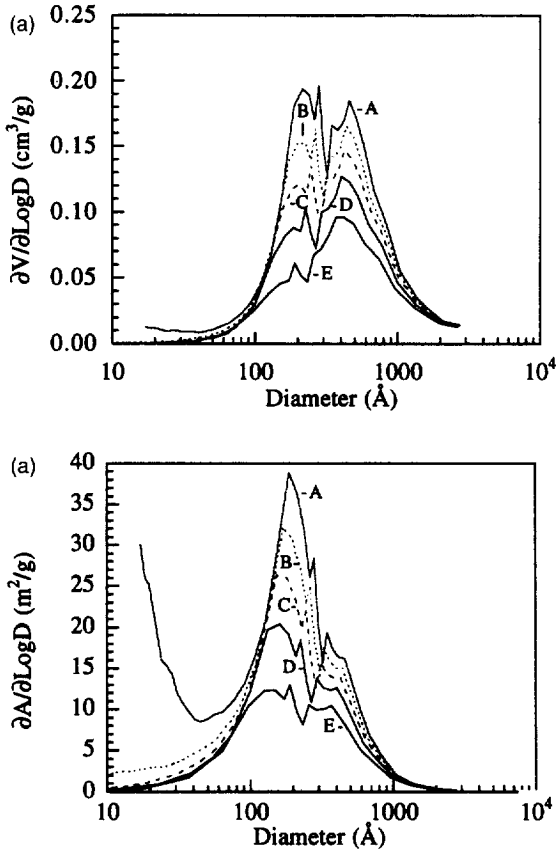


Fig. 4. Differential pore volume (a) and pore area (b) distributions predicted using the model of a smooth coating of uniform thickness (model 1). The pore volume distribution for uncoated zirconia particles is used as the basis for the calculations. Polymer loadings are expressed as g PBD/g $ZrO_2$: (A) 0, (B) 0.018, (C) 0.031, (D) 0.046, (E) 0.067.

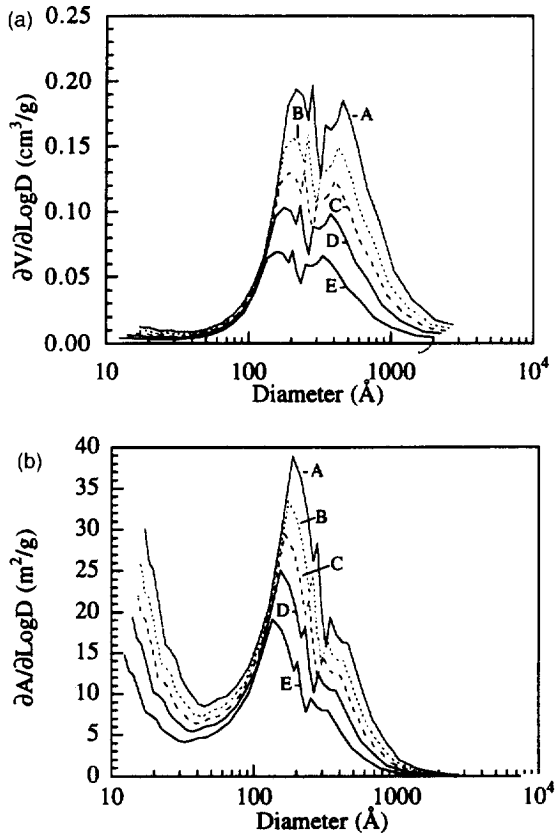


Fig. 5. Differential pore volume (a) and pore area (b) distributions predicted using the model of a smooth coating with a uniform volume fraction of polymer within the pores (model 2). The pore volume distribution for uncoated zirconia particles is used as the basis for the calculations. Polymer loadings are expressed as g PBD/g $ZrO_2$: (A) 0, (B) 0.018, (C) 0.031, (D) 0.046, (E) 0.067.

polymer lies flat against the surface (model 2). In contrast, with a polymer layer of uniform thickness (model 1), volume is lost from smaller pore much more quickly than from larger pores, and again, peaks shift toward smaller pore diameters with increased loading. The pore area distributions show similar trends. Note, however, that from volume distribution plots alone, one cannot say whether a shift in a peak towards smaller pore diameters indicates: (1) a surface layer which reduces the diameter of the pore or (2) a preference for polymer to reside in larger pores; some measure of the surface area change must be considered as well.

From the pore volume distribution plots and the

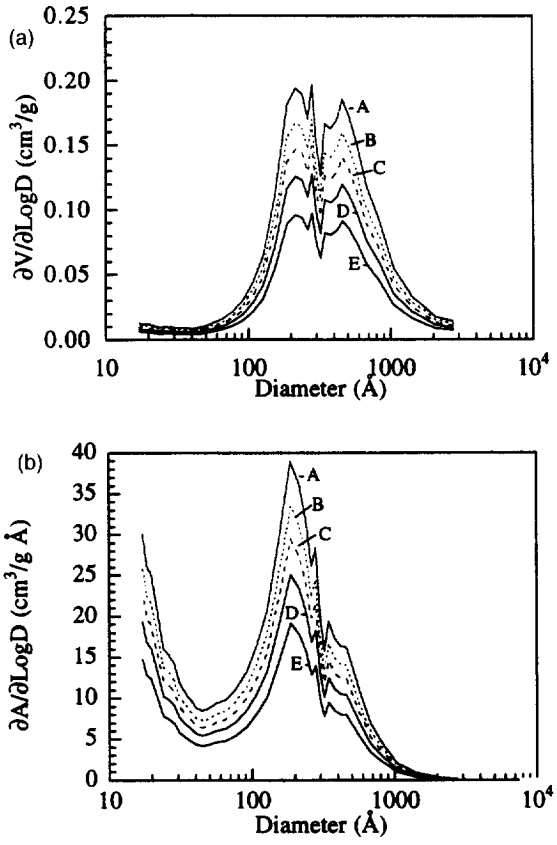


Fig. 6. Differential pore volume (a) and pore area (b) distributions predicted using the model of plugs with a uniform volume fraction of polymer within the pores (model 3). The pore volume distribution for uncoated zirconia particles is used as the basis for the calculations. Polymer loadings are expressed as g PBD/g $ZrO_2$: (A) 0, (B) 0.018, (C) 0.031, (D) 0.046, (E) 0.067.

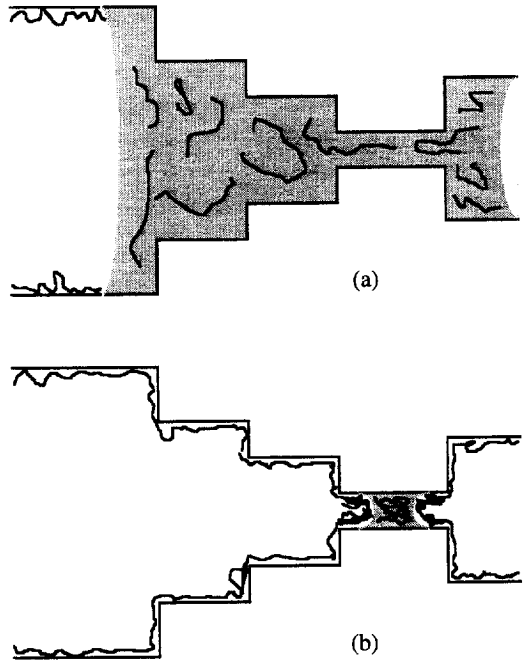


Fig. 7. Depiction of proposed mechanism for PBD deposition in porous zirconia. As the solvent is evaporated, leaving first from larger pores which are connected to the outer surface of the particle, the meniscus withdraws into smaller pores. As the meniscus withdraws, polymer deposits on the surface up to some critical amount (a). The excess polymer, which is not deposited, is carried with the receding meniscus into smaller pores. As solvent evaporates from the smallest pores in a cluster, the polymer has nowhere to go and is deposited there (b).

surface area measurements, it appears that for loadings of less than about 0.025 g PBD/g $ZrO_2$: (1) the amount of polymer within a pore of a given size is proportional to the pores volume and (2) the polymer remains relatively flat against the surface. By an approximate calculation, assuming a monolayer thickness of 1.5–3.5 Å (a range of estimates for the effective length of a carbon–carbon bond in a polymer backbone), a loading of 0.025 g PBD/g $ZrO_2$ would represent only 1/4 to 1/2 of a monolayer. At higher loadings, polymer preferentially gathers within the smaller pores. Based on this, we propose the following scenario for what is occurring during the coating procedure (Fig. 7). In the presence of the hexane solvent, the polybutadiene roughly equilibrates within the pore space to a uniform concentration. As the hexane is evaporated, leaving first from larger pores which are connected to the outer surface of the particle, the meniscus will withdraw into smaller pores. As the meniscus withdraws, polymer deposits on the surface up to some critical amount. The excess polymer, which is not deposited, is carried with the receding meniscus into smaller pores. As hexane evaporates from the smallest pores in a cluster, the polymer has nowhere to go and is deposited there. A more detailed, mechanistic model could qualitatively predict this behavior; however, it would not be possible to quantitatively predict the behavior for a specific system without detailed knowledge of the microscopic pore structure.

## 5. Conclusion

A series of pore volume distributions in conjunction with pore area distributions or measures of total pore surface area indicate how polymer occupies porous zirconia particles suitable for use as a support in reversed-phase liquid chromatography. We have compared experimental nitrogen adsorption data for PBD coatings on porous zirconia with three models which predict changes in pore size distribution for cylindrical pores under well-defined states of polymer distribution. These initial models are not mechanistic and do not predict the contributions of different physical mechanisms to the polymer distribution within the pore space; however, the results show that they have the potential to aid in interpreting experimental data. At low loadings, PBD appears to deposit in thin layers on the surface with no preference for large or small pores, similar to the behavior of model 2. At higher PBD loadings, the polymer deposits preferentially in smaller pores, similar to the behavior of model 3. This is in qualitative agreement with PBD coatings on porous silica.

## 6. Nomenclature

$a$: Diameter of uncoated pores [Å]
$A$: Total surface area of particles [$m^2/g$]
$d$: Diameter of coated pores [Å]
$f_V(a)$: Pore volume distribution as a function of uncoated pore diameter [$cm^3/g$ Å]
$f_A(a)$: Pore area distribution as a function of uncoated pore diameter [$m^2/g$ Å]
$g_V(a)$: Pore volume distribution as a function of uncoated pore diameter for logarithmic distribution [$cm^3/g$]
$g_A(a)$: Pore area distribution as a function of uncoated pore diameter for logarithmic distribution [$m^2/g$]
$S$: Ratio of polymer volume to pore volume of uncoated particles []
$V_0$: Total pore volume of uncoated particles [$cm^3/g$]
$V_1$: Total pore volume of particles [$cm^3/g$]
$\bar{V}_{PBD}$: Specific volume of polybutadiene [$cm^3/g$]
$W$: Polymer loading of polybutadiene [g PBD/g $ZrO_2$]
$\partial V/\partial D$: Pore volume distribution [$cm^3/g$ Å]
$\partial A/\partial D$: Pore area distribution [$m^2/g$ Å]
$\epsilon$: 2×Thickness of polymer layer

## Acknowledgments

This work was supported by grants GM 45988 from the National Institutes of Health and CHE 917029 from the National Science Foundation. D.H.R. gratefully recognizes the support of the National Institutes of General Medical Sciences through a Biotechnology Training Fellowship (IT32-GM08347). Thanks also go to the Surface Analysis Center at the University of Minnesota for instrumentation.

## References

[1] M. Petro and D. Berek, Chromatographia, 37 (1993) 549.
[2] A. Kurganov, V. Davankov and T. Isajeva, J. Chromatogr. A, 660 (1994) 97.
[3] G. Huhn and H. Müller, J. Chromatogr., 640 (1993) 57.
[4] A. Kurganov, O. Kuzmenko, V.A. Davankov, B. Eray, K.K. Unger and U. Trüdinger, J. Chromatogr., 506 (1990) 391.
[5] J.R. Garbow, J. Asrar and C.J. Hardiman, Chem. Mater., 5 (1993) 869.
[6] J. Nawrocki, M.P. Rigney, A.V. McCormick and P.W. Carr, J. Chromatogr. A, 657 (1993) 229.
[7] J. Nawrocki, C. Dunlap, P.W. Carr and J.A. Blackwell, Biotechnol. Prog., 10 (1994) 561.
[8] C. Dunlap, P.W. Carr and A.V. McCormick, Chromatographia, 42 (1996) 273.
[9] J.A. Blackwell and P.W. Carr, J. Chromatogr., 549 (1991) 59.
[10] M.H. Glavanovich and P.W. Carr, Anal. Chem., 66 (1994) 2584.
[11] C. McNeff, Q. Zhao and P.W. Carr, J. Chromatogr. A, 684 (1994) 201.
[12] C. McNeff and P.W. Carr, Anal. Chem., 67 (1995) 3886.
[13] M.P. Rigney, T.P. Weber and P.W. Carr, J. Chromatogr., 484 (1989) 273.
[14] L. Sun and P.W. Carr, Anal. Chem., 67 (1995) 2517.
[15] L. Sun and P.W. Carr, Anal. Chem., 67 (1995) 3717.
[16] C. Horváth and H.-J. Lin, J. Chromatogr., 149 (1978) 43.
[17] A.M. Lenhoff, J. Chromatogr., 384 (1987) 285.
[18] J. Li and P.W. Carr, Anal. Chem., submitted for publication.
[19] E.P. Barrett, L.G. Joyner and P.P. Halenda, J. Am. Chem. Soc., 73 (1951) 373.
[20] F.A.L. Dullien and V.K. Batra, Ind. Eng. Chem., 62 (1970) 25.

[21] K.K. Unger, in K.M. Gooding and F.E. Regnier (Editors), HPLC of Biological Macromolecules, Marcel Dekker, New York, 1990.
[22] J.H. Petropoulos, A.I. Liapis, N.P. Kolliopoulos, J.K. Petrou and N.K. Kanellopoulos, Bioseparation, 1 (1990) 69.
[23] C.F. Lorenzano-Porras, Ph.D. Thesis, University of Minnesota, Minneapolis, MN, 1995.
[24] L. Sun, M.J. Annen, C.F. Lorenzano-Porras, P.W. Carr and A.V. McCormick, J. Colloid Interface Sci., 163 (1994) 464.
[25] M. Hanson, B. Eray, K.K. Unger, A.V. Neimark, J. Schmid, K. Albert and E. Bayer, Chromatographia, 35 (1993) 403.